

AD-A098 424

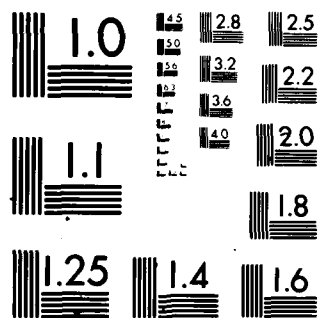
ROCKWELL INTERNATIONAL THOUSAND OAKS CA SCIENCE CENTER F/G 11/2
RESEARCH OF MICROSTRUCTURALLY DEVELOPED TOUGHENING MECHANISMS I--ETC(U)
MAR 81 F F LANGE N00014-77-C-0441

UNCLASSIFIED

SC5117.11TR

NL

END
DATE
FILMED
8-81
DTIC



MICROCOPY RESOLUTION TEST CHART
NATIONAL BUREAU OF STANDARDS 1963 A

AD A098424

LEVEL II



Rockwell International

Science Center
SC5117.11TR

14

Research of Microstructurally

Developed

TRANSFORMATION TOUGHENING

PART 4. FABRICATION, FRACTURE TOUGHNESS AND STRENGTH OF Al_2O_3/ZrO_2 COMPOSITES.

10 F.F./Lange

Structural Ceramics Group
Rockwell International Science Center
Thousand Oaks, California 91360

MAR. 81

11 Mar 81

12 21

ABSTRACT

15 N00014-77-C-0441

Three Al_2O_3/ZrO_2 composite series, containing 0, 2 and 7.5 mole % Y_2O_3 , were fabricated for fracture toughness determinations. Without Y_2O_3 additions, tetragonal ZrO_2 could only be retained up to ~10 volume % ZrO_2 ; additions of 2 m/o Y_2O_3 allowed full retention up to 60 v/o ZrO_2 . Cubic ZrO_2 was produced with additions of 7.5 m/o Y_2O_3 . Significant toughening and strengthening was achieved when tetragonal ZrO_2 was present.

DTIC
ELECTE

MAR 4 1981

1. Introduction

9 Trans. rept. no. 11
1 Dec 80-1 Apr 81, 5

In Part 1⁽¹⁾ of this series, the thermodynamics of a constrained phase transformation was presented, with particular reference to the size effect associated with retaining the high temperature phase. Part 2⁽²⁾ presented the theory concerning the contribution of the stress-induced transformation to fracture toughness. Part 3⁽³⁾ reported experimental observations concerning retention of tetragonal ZrO_2 and its contribution to fracture toughness for a series of materials fabricated in the ZrO_2 - Y_2O_3 system. The theory shows that both the critical inclusion size and the contribution to fracture toughness can be increased by choosing a constraining matrix with a higher elastic modulus relative to ZrO_2 .

389949

81 5

04 115

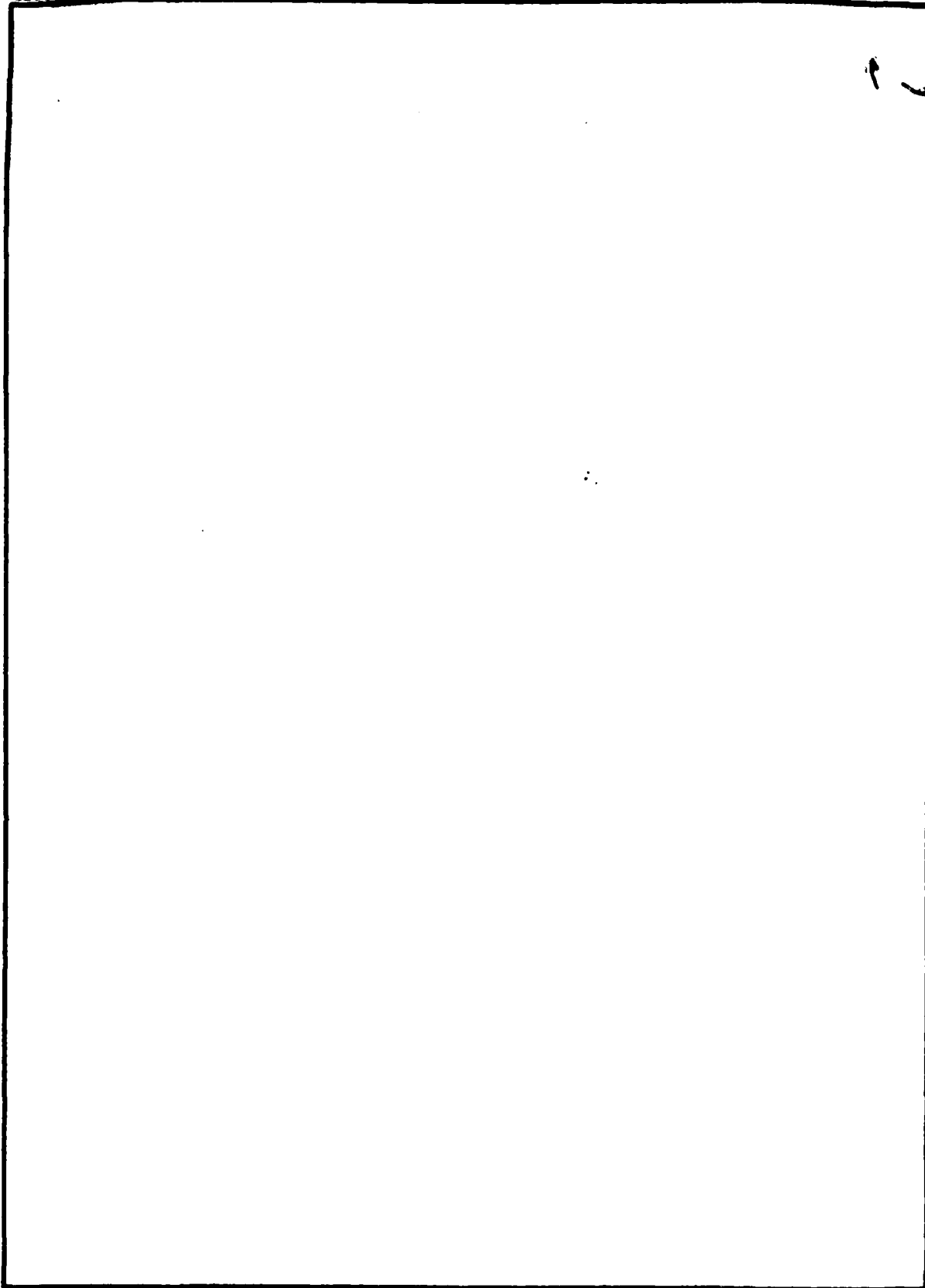
C2707A/jbs

This document has been approved
for public release and sales
distribution is unlimited.

DTIC FILE COPY

UNCLASSIFIED

SECURITY CLASSIFICATION OF THIS PAGE(When Data Entered)



UNCLASSIFIED

SECURITY CLASSIFICATION OF THIS PAGE(When Data Entered)

UNCLASSIFIED

SECURITY CLASSIFICATION OF THIS PAGE (When Data Entered)

REPORT DOCUMENTATION PAGE		READ INSTRUCTIONS BEFORE COMPLETING FORM
1. REPORT NUMBER	2. GOVT ACCESSION NO.	3. RECIPIENT'S CATALOG NUMBER
	AD A098424	
4. TITLE (and Subtitle)		5. TYPE OF REPORT & PERIOD COVERED
Research of Microstructurally Developed Toughening Mechanisms in Ceramics		Technical Report No. 11 12/01/80 through 04/01/81
7. AUTHOR(s)		6. PERFORMING ORG. REPORT NUMBER
F.F. Lange		SC5117.11TR ✓
9. PERFORMING ORGANIZATION NAME AND ADDRESS		8. CONTRACT OR GRANT NUMBER(s)
Rockwell International Science Center 1049 Camino dos Rios Thousand Oaks, CA 91360		N00014-77-C-0441 ✓
11. CONTROLLING OFFICE NAME AND ADDRESS		10. PROGRAM ELEMENT, PROJECT, TASK AREA & WORK UNIT NUMBERS
Director, Metallurgy Programs, Material Sciences Office of Naval Research, 800 N. Quincy Street Arlington, VA 22217		032-574(471)
14. MONITORING AGENCY NAME & ADDRESS (if different from Controlling Office)		12. REPORT DATE
		March 1981
		13. NUMBER OF PAGES
		21
		15. SECURITY CLASS. (of this report)
		Unclassified
		18a. DECLASSIFICATION/DOWNGRADING SCHEDULE
16. DISTRIBUTION STATEMENT (of this Report)		
Approved for public release; distribution unlimited		
17. DISTRIBUTION STATEMENT (of the abstract entered in Block 20, if different from Report)		
18. SUPPLEMENTARY NOTES		
19. KEY WORDS (Continue on reverse side if necessary and identify by block number)		
Fracture toughness, martensitic transformations, ZrO_2 , Al_2O_3 , phase transformation, strength		
20. ABSTRACT (Continue on reverse side if necessary and identify by block number)		
Three Al_2O_3/ZrO_2 composite series, containing 0, 2 and 7.5 mole % Y_2O_3 , were fabricated for fracture toughness determinations. Without Y_2O_3 additions, 2 m/o Y_2O_3 allowed full retention up to 60 v/o ZrO_2 . Cubic ZrO_2 was produced with additions of 7.5 m/o Y_2O_3 . Significant toughening and strengthening was achieved when tetragonal ZrO_2 was present.		

DD FORM 1 JAN 78 1473

EDITION OF 1 NOV 65 IS OBSOLETE

UNCLASSIFIED

SECURITY CLASSIFICATION OF THIS PAGE (When Data Entered)

389949 fm



The $\text{Al}_2\text{O}_3\text{-ZrO}_2$ system was chosen for this study because Al_2O_3 has approximately twice the elastic modulus of ZrO_2 (390 GPa vs 207 GPa) and both phases are chemically compatible with one another.⁽⁴⁾ Claussen⁽⁵⁾ has already demonstrated that $\text{Al}_2\text{O}_3/\text{ZrO}_2$ polycrystalline composites could be fabricated, and he also has demonstrated⁽⁶⁾ that tetragonal ZrO_2 could be retained in volume fractions up to 0.17. The intent of the present work was to fabricate a series of $\text{Al}_2\text{O}_3/\text{ZrO}_2$ composite materials from one end-member to the other and to retain the ZrO_2 in its tetragonal state. Initial studies indicated that within the range of fabrication parameters investigated, "pure" tetragonal ZrO_2 could only be retained in volume fractions < 0.10 . Based on theoretical considerations (Part 1) and retention studies in the $\text{ZrO}_2\text{-Y}_2\text{O}_3$ system (Part 3), it was found that additions of 2 m/o Y_2O_3 to the composite powders would allow the retention of the tetragonal phase to much greater volume fractions of ZrO_2 . Thus, this series of materials formed the principal base for investigating the contribution of the stress-induced phase transformation to fracture toughness and strength.

2. Experimental

2.1 Fabrication and Phase Identification

Three composite series were fabricated for this study: one containing pure ZrO_2 with volume fractions up to 0.20, one containing $\text{ZrO}_2 + 2 \text{ m/o } \text{Y}_2\text{O}_3^*$ in which tetragonal ZrO_2 was retained, and one containing $\text{ZrO}_2 + 7.5 \text{ m/o } \text{Y}_2\text{O}_3$ in which cubic ZrO_2 was obtained. The latter composite series was used for base

*m/o = mole %, v/o = volume %

tion For	GP&I	TAB	enced	Retention	tion/	ility Codes	and/or	-tal
	<input checked="" type="checkbox"/>	<input type="checkbox"/>	<input type="checkbox"/>	<i>Ret. base for</i>				



line information where transformation toughening was not a phenomena associated with the material's fracture mechanics.

Sub-micron powers were used.* Y_2O_3 was introduced as soluble yttrium nitrate.† Composite powders were mixed by ball-milling with methanol and Al_2O_3 balls in a plastic container. All powders were dried; those containing yttrium nitrate were calcined at $400^\circ C$ for 4 hrs. Densification was achieved by hot-pressing. Most Y_2O_3 containing compositions were hot-pressed at $1600^\circ C/2$ hrs; compositions containing 0.8 and 1.0 volume fraction $ZrO_2(+2$ m/o $Y_2O_3)$ were hot-pressed at $1400^\circ C$ in order to achieve a smaller grain size which allowed the retention of tetragonal ZrO_2 . The non-yttria composites were hot-pressed at $1500^\circ C$, again to achieve a smaller grain size for optimizing the retention of tetragonal ZrO_2 . The pure Al_2O_3 end-member was hot-pressed at $1400^\circ C$ to achieve a grain size comparable to the two-phase materials (the introduction of one end-member into the other limited grain growth).

Archimedes' technique was used to measure density of the 5 cm diameter billets. Specimens were cut, ground and polished§ prior to phase identification by x-ray diffraction analysis. Two-theta scans between 27° to 33° were used to estimate the tetragonal/monoclinic ZrO_2 ratio, and scans between 55° to 62° were used to confirm either the tetragonal or the cubic ZrO_2 phase.

* Al_2O_3 : Lindy B, Union Carbide Corp.; ZrO_2 : Zircar Corp.

†Research Chemicals Inc.

§Surface damage caused by cutting and grinding causes the surface to transform. Polishing decreases the depth of the transformed surface layer.



2.2 Mechanical Measurement

Young's modulus (E) of selected compositions was measured at room temperature by the resonance technique with two modes of vibration: flexural (9 kHz) and extensional (60 kHz).

The critical stress intensity factor (K_{IC}) was measured on polished specimens by using the indentation technique (20 kgm load) developed by Evans and Charles.⁽⁷⁾ Hardness (H) data was also obtained. Three measurements were made for each material.

Flexural strength measurements were obtained in four-point bending (inner span: 1.22 cm, outer span: 2.54 cm) on diamond cut specimens (approximately 0.32 × 0.32 cm cross sectional) finished with a 220 grit diamond grinding wheel.

3. Results

3.1 Fabrication and Phase Identification

Table 1 lists the fabrication conditions for the compositions reported here and their respective average properties. In the series which excluded Y_2O_3 , high proportions of tetragonal could only be retained up to ~ 10 v/o ZrO_2 . In the series containing 2 m/o Y_2O_3 , tetragonal ZrO_2 was fully retained up to ~ 60 v/o ZrO_2 . Cubic ZrO_2 was the only ZrO_2 structure observed in the series containing 7.5 m/o Y_2O_3 . No 4/Al oxide compounds were observed.

Lattice parameter measurements reported by Scott⁽⁸⁾ and confirmed in the present work are $a = 5.090\text{\AA}$, $c = 5.174\text{\AA}$ for the tetragonal (+2 m/o Y_2O_3)



structure and $a = 5.135\text{\AA}$ for the cubic structure. Using these values and the formulation $\text{Zr}_{1-x}\text{Y}_x\text{O}_{2-(x/2)}$, the theoretical densities for the tetragonal and cubic structures were calculated as 6.09 gm/cm^3 and 5.97 gm/cm^3 , respectively. Measured densities for the two composite series containing either the tetragonal or the cubic phases obeyed the rule of mixtures for the end-members (Al_2O_3 , $\rho = 3.98\text{ gm/cm}^3$), indicating that theoretical density was achieved during fabrication.

Figure 1 illustrates microstructures of the polished surfaces typical of the $\text{Al}_2\text{O}_3/\text{ZrO}_2$ composites (cracks present were purposely propagated from hardness indents). The observed agglomeration of the minor phase in occasional groups of 2 - 5 grains indicates that the dispersion could be improved. The average ZrO_2 grain size for the composite materials was dependent on the fabrication temperature, viz. $\sim 0.2\text{ }\mu\text{m}$ at 1400°C , $\sim 0.5\text{ }\mu\text{m}$ at 1500°C and $\sim 1\text{ }\mu\text{m}$ at 1600°C . The average grain size for the single phase end members was $\sim 2\text{ }\mu\text{m}$ for Al_2O_3 and $\sim 0.5\text{ }\mu\text{m}$ for ZrO_2 .

As reported in the Appendix, hot-pressed billets containing $> 30\text{ v/o}$ Al_2O_3 contained large surface cracks as observed by fluorescent dye penetration. Although small crack-free specimens could be cut and polished for K_{IC} measurements, larger bar specimens invariably contained one or more cracks, which restricted meaningful strength measurements to composites containing $< 30\text{ v/o}$ ZrO_2 .



SC5117.11TR

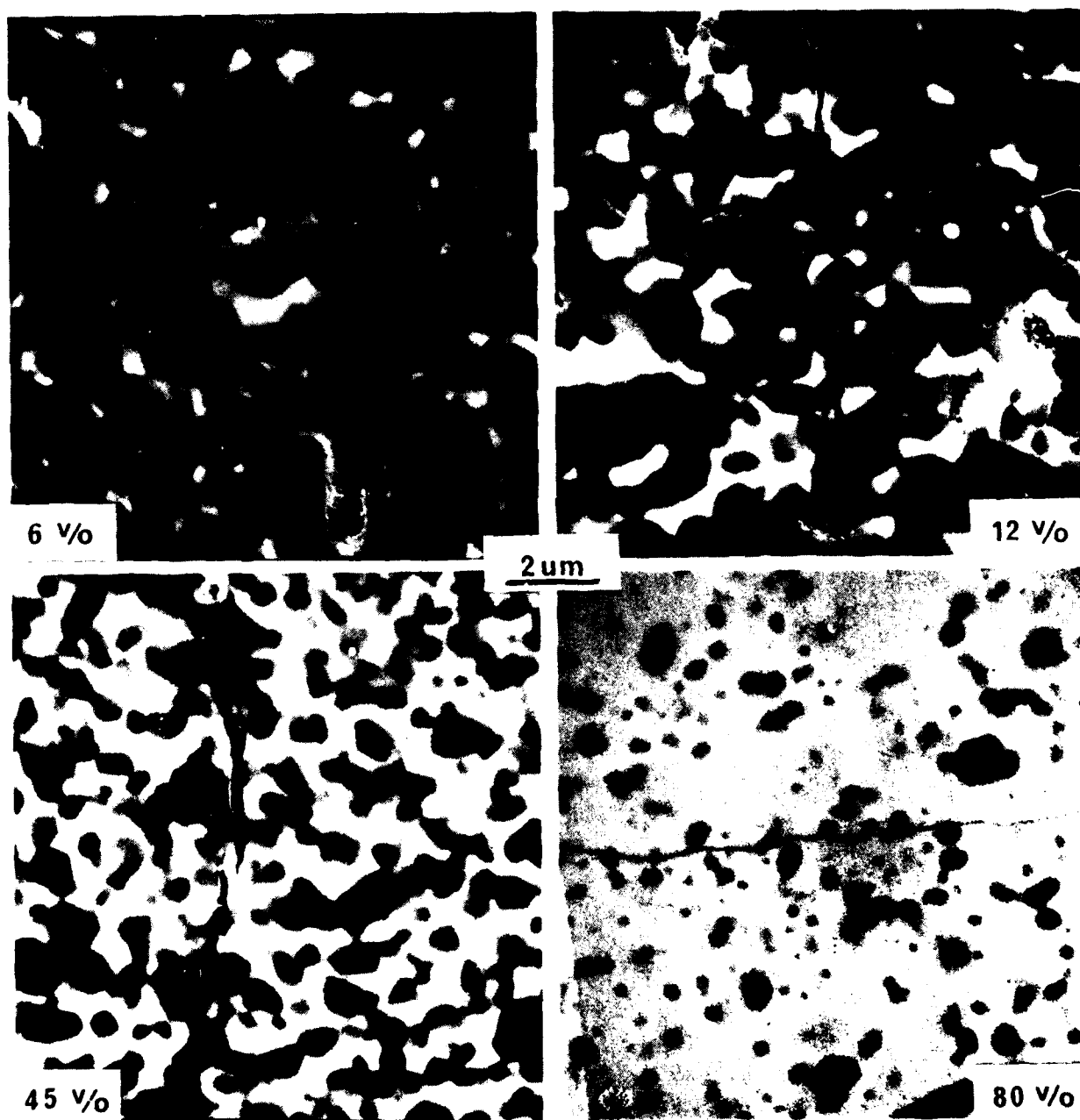


Fig. 1 SEM micrographs of polished surfaces of $\text{Al}_2\text{O}_3/\text{ZrO}_2$ (+2 m/o Y_2O_3) composites at ZrO_2 volume fractions of 0.063, 0.123, 0.45 and 0.80. Al_2O_3 is dark phase.



3.2 Hardness

Figure 2 illustrates the Vickers hardness (20 kgm) for the $\text{Al}_2\text{O}_3/\text{ZrO}_2$ (+2 m/o Y_2O_3) series, suggesting that the hardness obeys a linear rule of mixtures. The 20 v/o ZrO_2 (pure) composition had an exceptionally low hardness (see Table 1). Its high monoclinic content and friable nature suggested that it contained a high density of microcracks. SEM observations adjacent to the hardness indent in this material indicated that the indenter pushed the microcracked material aside as it extended into the interior.

3.3 Young's Modulus

Figure 3 reports the Young's modulus of the $\text{Al}_2\text{O}_3/\text{ZrO}_2$ (+2 m/o Y_2O_3) series obtained from the two resonance techniques.

3.4 Critical Stress Intensity Factor

Figure 4a reports K_{IC} as a function of composition for the two series containing Y_2O_3 . A considerable increase in fracture toughness could be achieved with the addition of the tetragonal ZrO_2 (viz. the 2 m/o Y_2O_3 series). In contrast, the addition of cubic ZrO_2 lowered the fracture toughness (viz. the 7.5 m/o Y_2O_3 series). Figure 4b shows that the peak in K_{IC} for the series that excluded Y_2O_3 corresponds to the maximum retention of the tetragonal phase in this series.

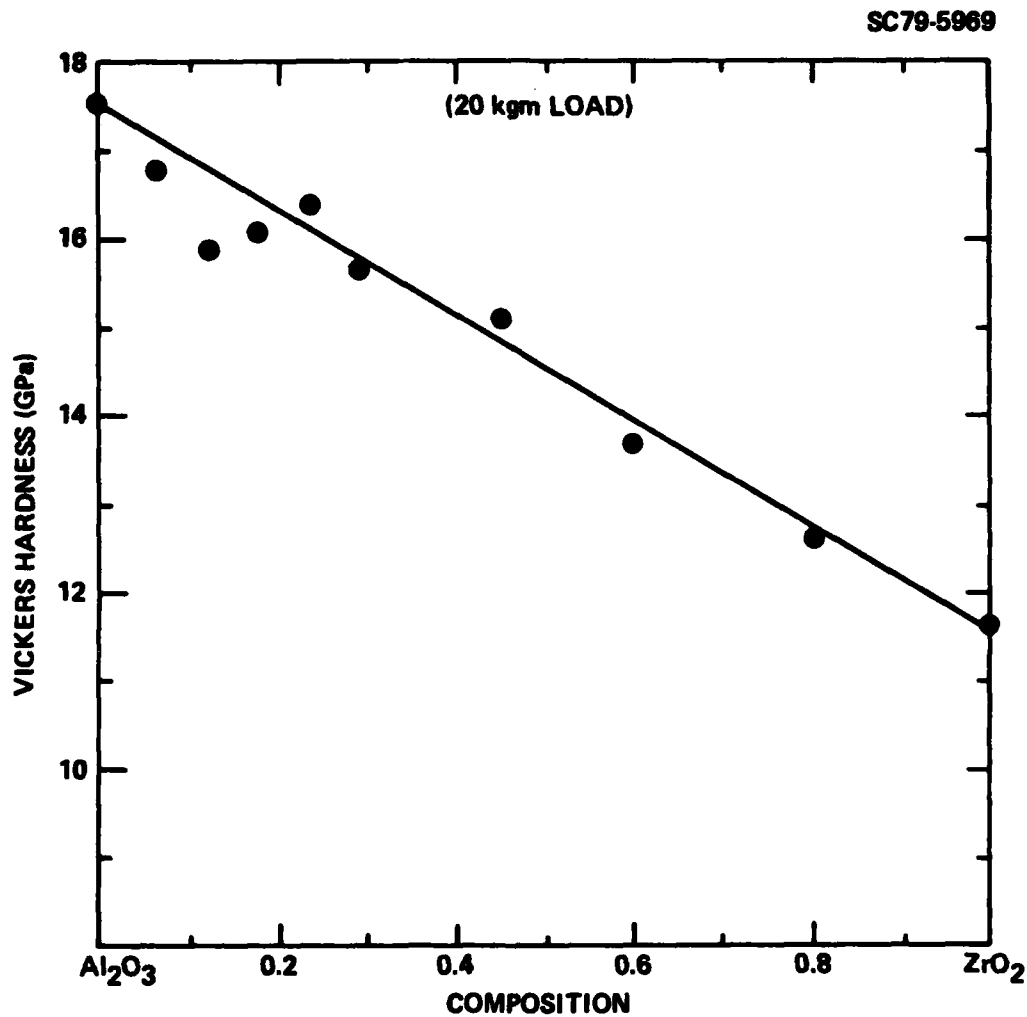


Fig. 2 Vicker's hardness (measured at 20 kgm) for the Al₂O₃/ZrO₂ (+2 m/o Y₂O₃) composite series.

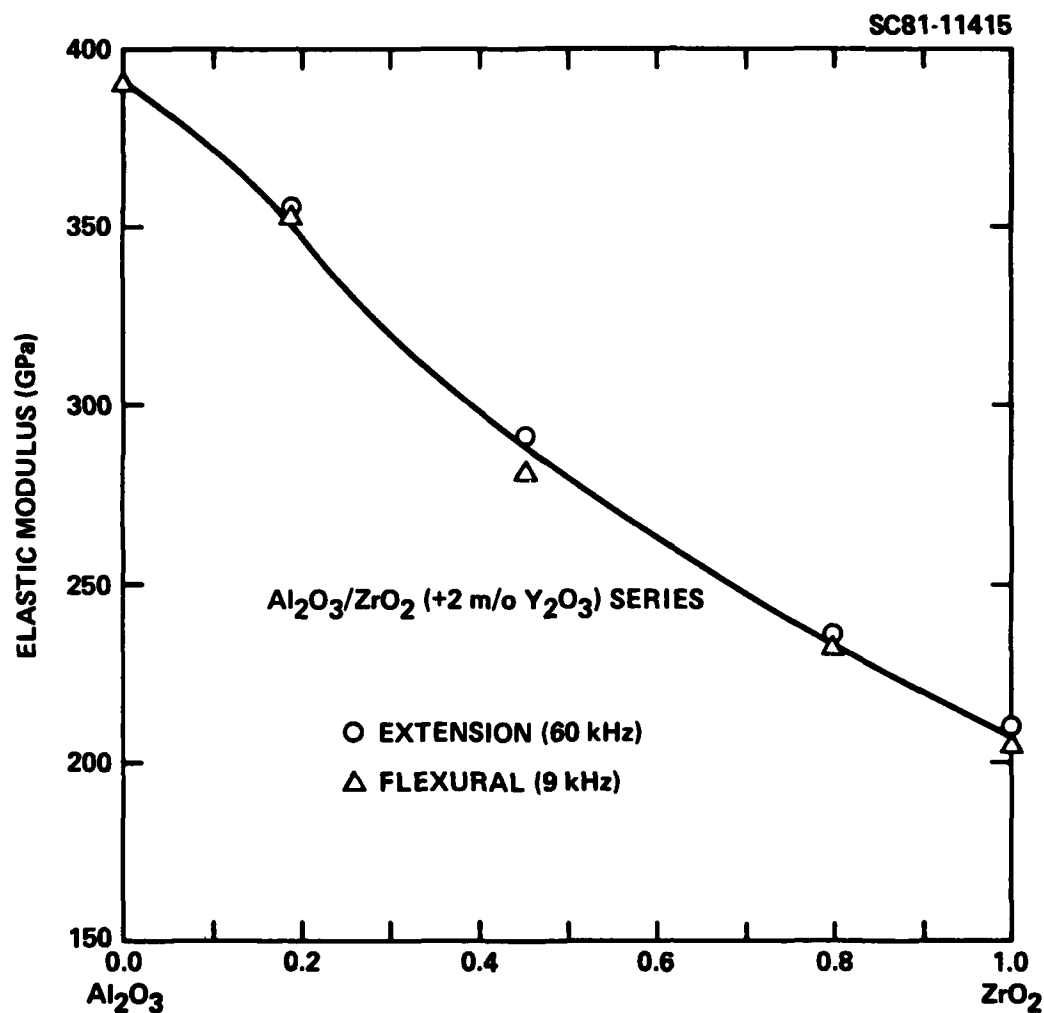


Fig. 3 Young's modulus vs composition for the $\text{Al}_2\text{O}_3/\text{ZrO}_2$ (+2 m/o Y_2O_3) series.

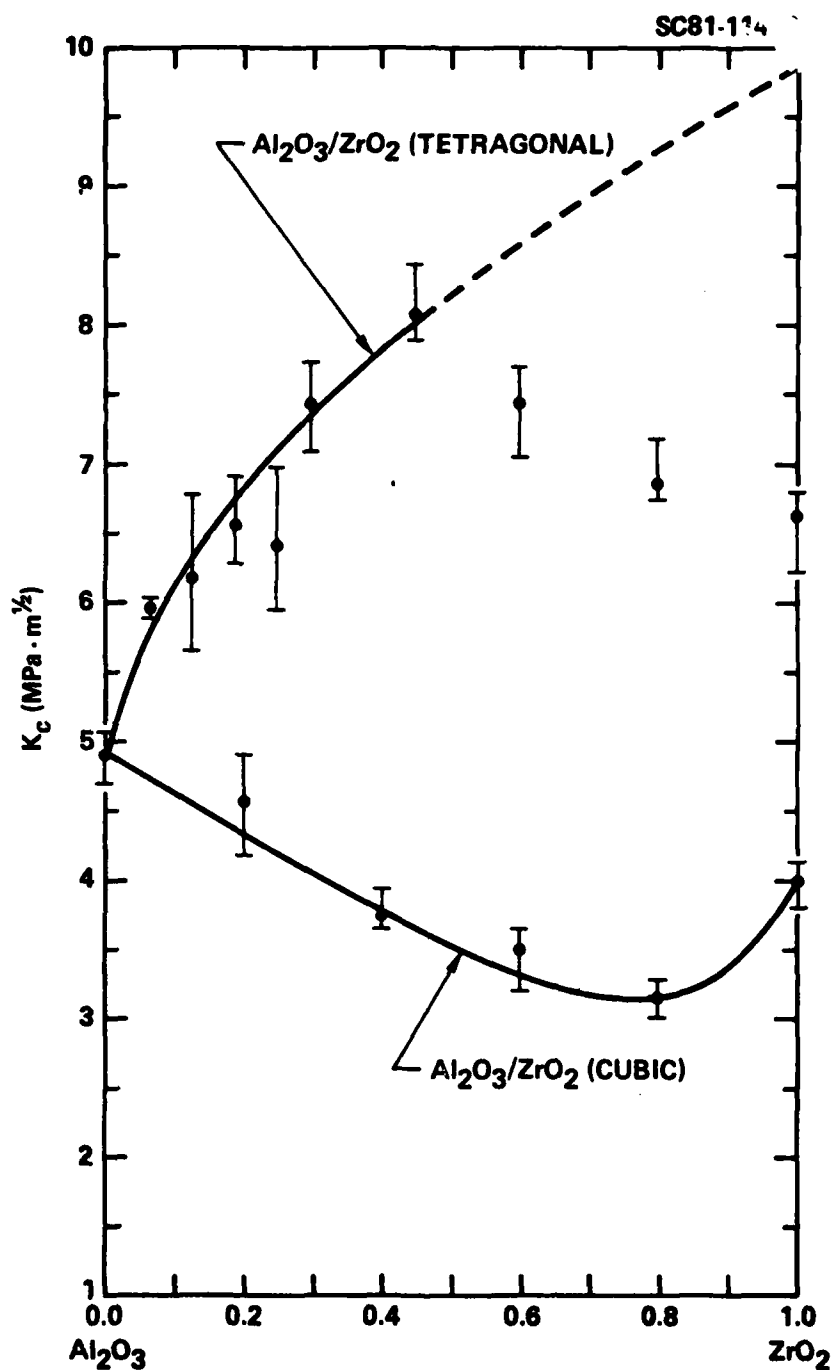


Fig. 4 a) Critical stress intensity factor vs composition for the $\text{Al}_2\text{O}_3/\text{ZrO}_2$ (+2 m/o Y_2O_3) (circles) and the $\text{Al}_2\text{O}_3/\text{ZrO}_2$ (+7.5 m/o Y_2O_3) series (squares).



SC79-5972

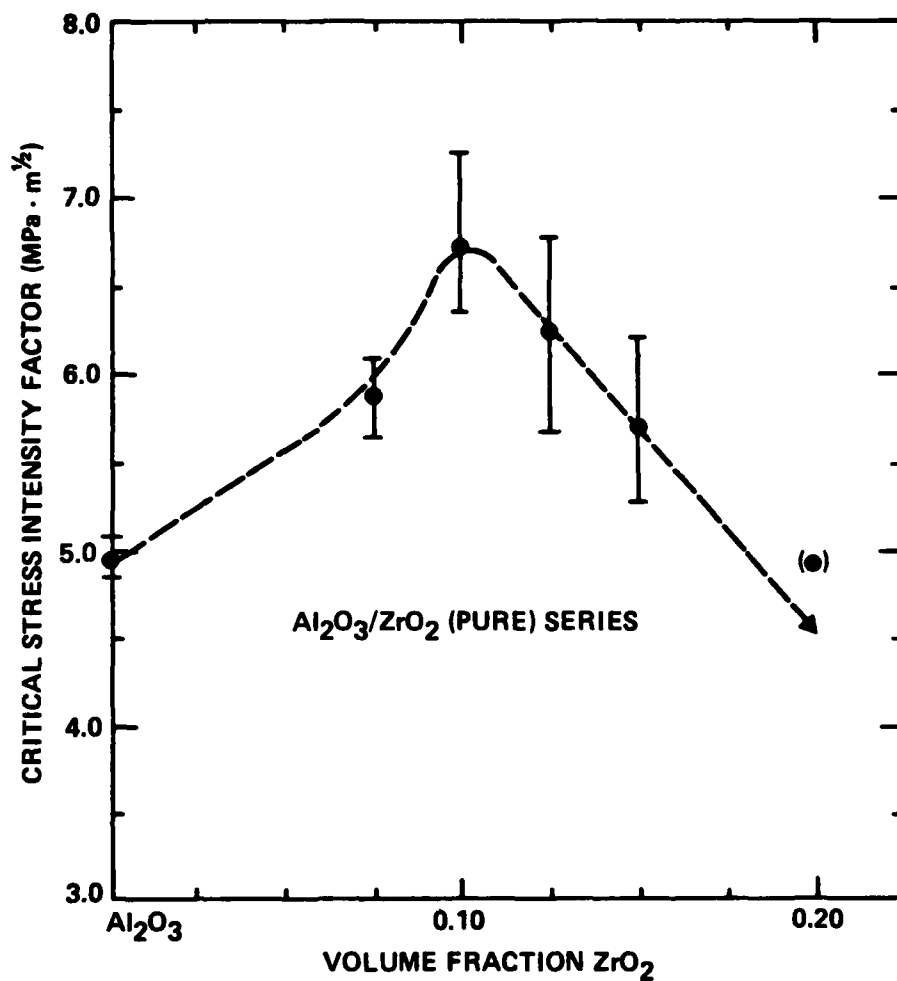


Fig. 4 b) Critical stress intensity factor vs composition for the Al₂O₃/ZrO₂ (pure) series.



3.5 Strength

Flexural strength determinations for the series containing 2 m/o Y_2O_3 are shown in Fig. 5. Since it is known that surface grinding can result in compressive surface stresses in these types of materials, a set of specimens were annealed at 1300°C prior to testing to eliminate the transformed surface layer. Annealing resulted in a lower average strength. It is interesting to note that significant strengthening of Al_2O_3 can be achieved by adding the tetragonal ZrO_2 toughening agent.

4. Discussion

4.1 Retention of Tetragonal ZrO_2

Part 1 of this series showed that the critical grain size for retaining the high temperature, tetragonal structure of ZrO_2 could be increased by increasing the elastic modulus of the constraining matrix and by alloying to decrease the chemical free energy change. Data presented here are consistent with these theoretical conclusions. Namely, without Y_2O_3 additions, retention of tetragonal ZrO_2 became more difficult as the elastic modulus of the composite decreased. Additions of 2 m/o Y_2O_3 resulted in phase retention to much large ZrO_2 volume fractions, despite the decreased modulus and larger grain size. Part 3 of this series showed that the critical grain size for ZrO_2 (+2 m/o Y_2O_3) was $\sim 0.2 \mu m$ when the constraining matrix was ZrO_2 . The current study shows that the critical grain size can be increased to at least $1 \mu m$ with the higher modulus of the Al_2O_3/ZrO_2 constraining matrix. Also note that as the composition approached the ZrO_2 end-member, the fraction of retained tetragonal phase decreased.



SC79-5971

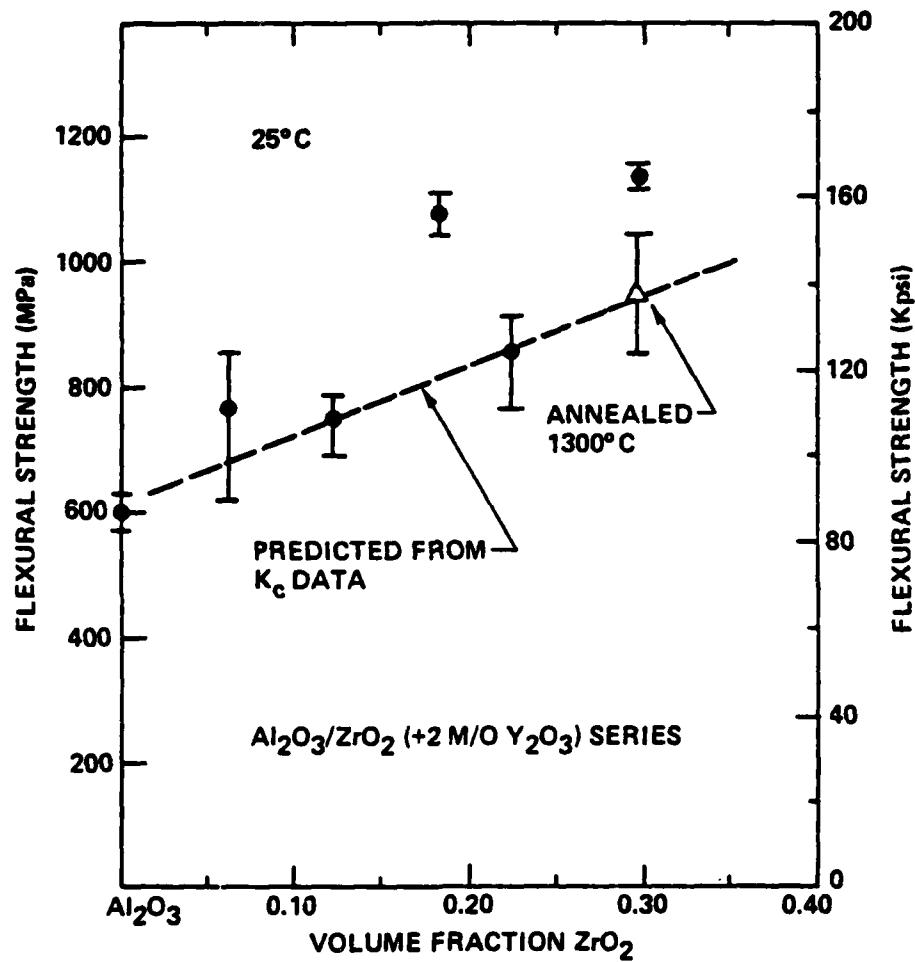


Fig. 5 Flexural strength vs composition for the $\text{Al}_2\text{O}_3/\text{ZrO}_2$ (+2 m/o Y_2O_3) series.



4.2 Fracture Toughness

Fracture toughness data presented in Figure 4 clearly illustrates that the tetragonal phase is the toughening agent. When cubic ZrO_2 is incorporated into Al_2O_3 , the toughness decreases. This may be a result of residual stresses associated with differential thermal expansion. Data for the series which excluded Y_2O_3 indicate that the toughness decreased with increasing monoclinic content.

Part 2 of this series presented an expression for K_C :

$$K_C = \left[K_0^2 + \frac{2(|\Delta G^C| - \Delta U_{se} f) E_C V_1 R}{(1 - \nu_C^2)} \right]^{1/2}, \quad (1)$$

where K_0 is the critical stress intensity factor for the composite without the transformation toughening phenomena, $(|\Delta G^C| - \Delta U_{se} f)$ is the work done per unit volume to stress-induce the transformation, E_C and ν_C are the elastic properties of the composite, V_1 is the volume fraction of the tetragonal ZrO_2 and R is the size of the transformation zone adjacent to the crack. By using the measured values of K_C for the series containing the tetragonal ZrO_2 , the values of K_0 obtained from the series containing cubic ZrO_2 , E_C from Fig. 3, $\nu_C = 0.25$ and assuming that $R = 1 \mu m$ (i.e., the average grain size for this series when $V_1 < 60$ v/o ZrO_2), the average value of $(|\Delta G^C| - \Delta U_{se} f)$ was calculated as 188 MJ/m^2 for compositions containing < 60 v/o tetragonal ZrO_2 . The agreement of the experimental data with this value is shown by the solid line drawn through the Al_2O_3/ZrO_2 (tetragonal) data. Although this value is in good agreement with that calculated in Part 3 for the $ZrO_2 + 3 \text{ m/o } Y_2O_3$ material (188 MJ/m^3 vs 176 MJ/m^3), this agreement may be fortuitous since the magnitude of the terms in



$(|\Delta G^C| - \Delta U_{se})$ are expected to be different for the two systems. Namely, $|\Delta G^C|$ should be greater for the $ZrO_2 + 2$ m/o Y_2O_3 composition relative to the $ZrO_2 + 3$ m/o Y_2O_3 composition, and ΔU_{se} should be greater for the higher modulus Al_2O_3/ZrO_2 constraining matrix relative to constraint with ZrO_2 alone.

As shown in Fig. 4a, good agreement between theory (Eq. 1) and data is obtained for compositions containing < 0.45 v/o ZrO_2 . Poor agreement is obtained at higher volume fractions. This lack of agreement may be due to the lack of total retention of the tetragonal ZrO_2 when $V_1 > 60$ v/o, the smaller grain size of the higher ZrO_2 compositions and/or a compositional difference due to the apparent oxygen deficiency of the ZrO_2 (see the Appendix).

4.3 Strength

The strength data presented in Fig. 5 has been analyzed to determine its dependence on the experimental K_c values. In this analysis, it was assumed that the crack size distribution responsible for failure remained unchanged from material to material. With this assumption, the strength of each material should be related by their respective critical stress intensity factors:

$$\sigma_2 = \frac{K_2}{K_1} \sigma_1 \quad (2)$$

This relation was used with the average strength and K_c for the pure Al_2O_3 to obtain the broken line in Fig. 5. As shown, three of the original five sets of data were in good agreement with this analysis, but two of the data sets (viz. $V_p = 0.182$ and 0.295) were higher than predicted.



Pascoe and Garvie⁽⁹⁾ have shown that surface compressive stress arises in materials containing metastable, tetragonal ZrO_2 when the transformation at the surface is induced by an abrasion process. The volume increase associated with transformed surface layer gives rise to the compressive stresses. Since each set of strength specimens was independently surface ground, it was suspected that several of these sets (the two that resulted in the higher values) may have received surface damage to impart sufficient surface compressive stresses to increase their strength. To test this hypothesis, a small task was initiated to examine the effect of surface abrasion on strength. Although the principal results of this task will be reported elsewhere,⁽¹⁰⁾ it was shown that when the abrasively ground specimens were annealed at $1300^\circ C$ to eliminate the transformed surface layer, the average strength was lowered to that expected from Eq. (2). These data are shown by the open triangle in Fig. 5.

It can be concluded that the strength of the Al_2O_3/ZrO_2 (+2 m/o Y_2O_3) composite materials increases proportionally to their increase in K_c as expected. Additional strengthening can be obtained by compressive stressing the surfaces through abrasion. Studies are currently underway to characterize and optimize the abrasion phenomena.



APPENDIX:
FORMATION OF SURFACE CRACKS DURING THE HOT-PRESSING
OF $\text{Al}_2\text{O}_3/\text{Al}_2\text{O}_3$ COMPOSITES

As indicated in the text, $\text{Al}_2\text{O}_3/\text{ZrO}_2$ composites containing > 30 v/o ZrO_2 hot-pressed in graphite dies were observed to contain large surface cracks. Although the exact cause of the stresses that give rise to these cracks is beyond the scope of the present work, observations do exist to indicate a probable cause.

The color of hot-pressed $\text{Al}_2\text{O}_3/\text{ZrO}_2$ composite billets changes from a light grey to black as the ZrO_2 volume fraction increased to 1. A color gradient also exists within a sectioned billet, darker on the outside, lighter near the center. This color gradient indicates a compositional gradient. Black ZrO_2 can also be produced at high temperatures in vacuum, and ZrO_2 is known to lose oxygen in high temperature, low oxygen environments.

XRD examination did not reveal phases other than the ZrO_2 structures indicated in the text (Table 1). Surface and interior phases were the same (precise lattice parameter measurements were not performed).

Oxidation in air at 1300°C transformed the grey to black specimens to pure white. Sectioned, oxidized specimens would reveal a dark core for short oxidation periods. Oxidation resulted in moderate to severe surface spalling for compositions containing > 30 v/o ZrO_2 . The 100 v/o ZrO_2 specimens could be completely oxidized in 15 minutes at 750°C due to severe cracking.



The above evidence suggests that the dark color is consistent with an oxygen deficient ZrO_2 . Ruh and Garrett⁽¹¹⁾ have shown that the oxygen deficient ZrO_2 has a smaller molar volume. Thus, a gradient in the oxygen content of the ZrO_2 from the billet surface to its interior would result in surface tensile stresses at the fabrication temperature. With a sufficient volume fraction of ZrO_2 (e.g., > 30 v/o), these tensile stresses could be significant enough to produce surface cracks. Likewise, oxidation would increase the molar volume of the depleted phase to produce surface compressive stresses and surface spalling.⁽¹²⁾

ACKNOWLEDGEMENTS

The careful technical services of M.G. Metcalf are deeply appreciated. The author also wishes to acknowledge the valuable discussions with D.R. Clarke and D.J. Green. Thanks are due B.R. Tittmann and E.H. Cirlin for the elastic modulus measurements. This work was supported by the Office of Naval Research under Contract N00014-77-C-0441.



REFERENCES

1. F.F. Lange, "Part 1, Size Effects Associated with Constrained Phase Transformations."
2. F.F. Lange, "Part 2, Contribution to Fracture Toughness."
3. F.F. Lange, "Part 3, Experimental Observations in the $ZrO_2 - Y_2O_3$ System."
4. E.M. Levin, C.R. Robbins and H.F. McMurdie, Phase Diagrams for Ceramists, 1969 Supplement, The American Ceramic Soc., 1969.
5. N. Claussen, "Fracture Toughness of Al_2O_3 with an Unstabilized ZrO_2 Dispersion Phase," J. Am. Ceram. Soc., 59, 49 (1976).
6. N. Claussen, "Stress-Induced Transformation of Tetragonal ZrO_2 Particles in Ceramic Matrices," J. Am. Ceram. Soc., 61, 85 (1978).
7. A.G. Evans and E.A. Charles, "Fracture Toughness Determinations by Indentation," J. Am. Ceram. Soc. 59, 371 (1976).
8. H.G. Scott, "Phase Relations in the Zirconia-Yttria System," J. Mat. Sci., 10, 1527 (1975).
9. R.T. Pascoe and R.C. Garvie, Ceramic Microstructures '76, ed. by R.M. Fulrath and J.A. Pask, Westview Press p. 774 (1977).
10. D.J. Green and F.F. Lange, to be published.
11. R. Ruh and H.J. Garrett, "Nonstoichiometry of ZrO_2 and its Relation to Tetragonal-Cubic Inversion in ZrO_2 ," J. Amer. Ceram. Soc., 50, 257 (1967).
12. F.F. Lange, "Compressive Surface Stresses Developed in Ceramics by an Oxidation-Induced Phase Change," J. Am. Ceram. Soc., 63, 38 (1980).



Rockwell International

Science Center

SC5117.11TR

Table 1
FABRICATION CONDITIONS, PHASE CONTENT AND PROPERTIES OF $\text{Al}_2\text{O}_3/\text{ZrO}_2$ COMPOSITES

v/o ZrO_2	m/o Y_2O_3	Fabrication Condition	Density (gm/cm^3)	% ZrO_2^* Phrase	H (GPa)	E (GPa)	K_C ($\text{MPa}\cdot\text{m}^{1/2}$)
$\text{Al}_2\text{O}_3/\text{ZrO}_2$ (+2 m/o Y_2O_3) Series							
0	-	1400°C/2 hr	3.98	-	17.6	390	4.89
6	2	1600°C/2 hr	4.12	100t	16.8	-	5.97
12.3	2	1600°C/2 hr	4.26	100t	15.9	-	6.22
18.2	2	1600°C/2 hr	4.38	100t	16.1	356	6.58
23.9	2	1600°C/2 hr	4.50	100t	16.4	-	6.38
29.5	2	1600°C/2 hr	4.62	100t	15.7	-	7.43
45.0	2	1600°C/2 hr	4.89	trm	15.1	291	8.12
60.0	2	1600°C/2 hr	5.24	~95t	13.7	-	7.45
80.0	2	1400°C/2 hr	5.57	~85t	12.6	237	6.79
100.0	2	1400°C/2 hr	6.01	~80t	11.6	210	6.62
$\text{Al}_2\text{O}_3/\text{ZrO}_2$ (pure) Series							
7.5	-	1500°C/2 hr	4.12	~90t	17.2	-	5.88
10.0	-	1500°C/2 hr	4.15	~80t	15.8	-	6.73
12.5	-	1500°C/2 hr	4.22	~70t	16.9	-	6.21
15.0	-	1500°C/2 hr	4.25	~50t	17.3	-	5.71
20.0	-	1600°C/2 hr	-	<20t	10.1	-	(5.25)
$\text{Al}_2\text{O}_3/\text{ZrO}_2$ (+7.5 m/o Y_2O_3) Series							
20.0	7.5	1600°C/2 hr	4.46	100c	15.8	-	4.54
40.0	7.5	1600°C/2 hr	4.89	100c	15.9	-	3.75
60.0	7.5	1600°C/2 hr	5.28	100c	15.0	-	3.50
80.0	7.5	1600°C/2 hr	5.63	100c	14.3	-	3.14
100.0	7.5	1600°C/2 hr	5.95	100c	11.4	-	3.90

t = tetragonal

c = cubic

trm = trace monoclinic

